International Journal of Pharmaceutics 393 (2010) 176–184

Contents lists available at ScienceDirect

International Journal of Pharmaceutics

journal homepage: www.elsevier.com/locate/ijpharm

Pharmaceutical Nanotechnology

Nanoparticles with dextran/chitosan shell and BSA/chitosan core—Doxorubicin loading and delivery

Jianing Qi[a], Ping Yao[a,*], Fen He[b], Chuiliang Yu[b], Chong Huang[b]

[a] Key Laboratory of Molecular Engineering of Polymer and Department of Macromolecular Science, Fudan University, 220 Handan Road, Shanghai 200433, China
[b] National Pharmaceutical Engineering Research Center, Shanghai 201203, China

ARTICLE INFO

Article history:
Received 4 December 2009
Received in revised form 4 March 2010
Accepted 31 March 2010
Available online 8 April 2010

Keywords:
Albumin
Chitosan
Dextran
Doxorubicin
Drug delivery
Nanoparticles

ABSTRACT

Biocompatible bovine serum albumin (BSA)–dextran–chitosan nanoparticles were fabricated by heating the mixture of chitosan and BSA–dextran conjugates by virtue of the electrostatic attraction between BSA and chitosan as well as the gelation of BSA. The BSA–dextran conjugates were prepared by Maillard reaction. The nanoparticles were characterized by light scattering, ζ-potential, atomic force microscopy and pyrene fluorescence. The nanoparticles having a spherical shape and hydrodynamic diameters of 130–230 nm are stable in physiological condition. Doxorubicin can be effectively loaded into the nanoparticles after changing the pH of their mixture to 7.4 by virtue of the electrostatic and hydrophobic interactions between the nanoparticles and doxorubicin. The antitumor effects of doxorubicin loaded nanoparticles were investigated by the tumor inhibition and survivability of murine ascites hepatoma H22 tumor-bearing mice. The loaded nanoparticles can largely decrease the toxicity of doxorubicin and significantly increase the survivability of the tumor-bearing mice.

1. Introduction

Doxorubicin is widely used in chemotherapy due to its efficacy in fighting a wide range of cancers. The injury to non-targeted tissues often complicates cancer treatment by limiting doxorubicin dosage and diminishing the quality of patients' life during and after doxorubicin treatment (Carvalho et al., 2009). Nano-sized delivery systems of doxorubicin are a promising approach to increase its antineoplastic efficacy and lower its side-effects by site-specific drug delivery via active or passive targeting mechanism (Choi et al., 2009; Minotti et al., 2004). Doxorubicin has been loaded in various nanoparticles by chemical conjugation and/or physical entrapment (Kratz, 2007; Li and Wallace, 2008; Janes et al., 2001; Mitra et al., 2001; Son et al., 2003; Tan et al., 2009).

A "stealth" property is necessary for a nanoparticle shell for the purpose of avoiding reticuloendothelial recognition and subsequent elimination, and enabling passive accumulation of the nanoparticle in tumor (Gref et al., 1994; Otsuka et al., 2003; Patil et al., 2008). Currently, the most considered strategy relies on the immobilization of a poly(ethylene glycol) (PEG) corona onto the particle's surface (Gabizon et al., 2003; Patil et al., 2008; Wattendorf and Merkle, 2008). Polysaccharide, such as dextran, can also provide a nanoparticle with a stealth property and decrease the adsorption of plasma protein (Lemarchand et al., 2004; Passirani et al., 1998). Several dextran-coated nanoparticles, mainly in cancer imaging, have been reported, including their abilities to increase the circulation time in bloodstream and to target specific tumor tissues (Lemarchand et al., 2004; Park et al., 2009). Recently, Choi et al. reported doxorubicin encapsulated core–shell nanoparticles of poly(DL-lactide-co-glycolide) grafted-dextran copolymer and their antitumor activity *in vitro* and *in vivo* (Choi et al., 2009). The study shows that the nanoparticles with dextran shell are promising vehicles for antitumor drug delivery.

Chitosan, a biomaterial used in pharmaceuticals, has several advanced properties including bioadhesive nature (Tan et al., 2009). Chitosan displays a growth-inhibitory effect on bladder tumor cells (Hasegawa et al., 2001). Chitosan nanoparticles formed by coacervation between chitosan and sodium tripolyphosphate exhibit a stronger antitumor effect on human hepatoma cell line BEL7402 than chitosan molecules both *in vitro* and *in vivo* (Qi et al., 2007). Various doxorubicin chitosan nanoparticles have been reported (Hu et al., 2007; Tan et al., 2009), such as hydrophobic modification of chitosan with oleoyl chloride followed by oil/water emulsification with doxorubicin (Zhang et al., 2007) and synthetic conjugation of doxorubicin to glycol–chitosan followed by doxorubicin entrapment by oil/water emulsification (Son et al., 2003).

Albumin is a natural carrier of hydrophobic molecules, which realizes transport and distribution of many molecules and metabolites as well as many diverse drugs (Purcell et al., 2000). Human serum albumin (HSA) may also play a role in preferential intra-

* Corresponding author. Tel.: +86 21 65642964; fax: +86 21 65640293.
E-mail address: yaoping@fudan.edu.cn (P. Yao).

0378-5173/$ – see front matter © 2010 Elsevier B.V. All rights reserved.
doi:10.1016/j.ijpharm.2010.03.063

tumoral accumulation of paclitaxel (Desai et al., 2006). The hematological, cardiac, and testicular toxicities of doxorubicin can be effectively reduced by binding the drug to HSA nanoparticles (Pereverzeva et al., 2007). Dreis et al. recently reported the preparation of doxorubicin-loaded HSA nanoparticles (Dreis et al., 2007). In their study, doxorubicin can be loaded to HSA nanoparticles either by adsorption to the nanoparticles' surface or by incorporation into the particle matrix. Doxorubicin loading to HSA carrier system does not result in a reduced biological activity; the inhibition of cell growth is comparable or even better compared to a doxorubicin control solution. Yokoe et al. reported that recombinant HSA/PEG liposomal doxorubicin has longer blood-circulating property and higher therapeutic index than PEG liposomal doxorubicin (Yokoe et al., 2008).

Bovine serum albumin (BSA) is an abundant and low-cost protein having a molecular weight of 66 kDa. The gelation property and mechanism of BSA on heating have been reported (Boye et al., 1996; Ferry, 1948). This thermally induced gelation is a sequential process, which involves heat-induced unfolding followed by protein–protein interactions. The inter-protein interactions involve hydrogen bonding, electrostatic and hydrophobic interactions, and disulfide–sulfydryl interchange reaction. In this study, we utilized the heat-induced gelation of BSA to fabricate stable nanoparticles having a structure of chitosan/dextran shell and BSA/chitosan core. The purpose of this study is to develop a simple, green and low-cost process that produces the nanoparticles having the advantages of chitosan, dextran and albumin mentioned above. The antitumor effects of doxorubicin loaded nanoparticles were investigated through the tumor inhibition and survivability of murine ascites hepatoma H22 tumor-bearing mice.

2. Materials and methods

2.1. Materials

Doxorubicin hydrochloride (99.0%) was from Zhejiang Hisun Pharmaceutical Co. Ltd. Chitosan with molecular weight (M_w) of 50 kDa and deacetylation degree of 95.5% was obtained from Jinan Haidebei Marine Bioengineering Co. Chitosan (M_w 80–190 kDa, deacetylation degree 85%) and sulforhodamine B (SRB) were from Sigma. Dextran (M_w 62 kDa) and BSA (fraction V, 99%) were supplied by Amresco Inc. RPMI-1640 cell culture medium was purchased from GIBCO BRL Life Technologies Inc. Calf serum was from Hangzhou Sijiqing Biological Engineering Materials Co., Ltd. All other reagents were analytical grade. All solutions were prepared by deionized water which was filtered by 0.45 μm pore size filter to remove dust and bacteria.

2.2. BSA–dextran conjugate preparation

BSA and dextran were dissolved together in water with a desired molar ratio. The pH of the solution was adjusted to 7.1 with NaOH solution, then, the mixture solution was lyophilized. The lyophilized powder reacted at 60 °C and 79% relative humidity in a desiccator containing saturated KBr solution for 24 h. The resultant products were kept at −20 °C before use.

2.3. BSA–dextran–chitosan nanoparticle preparation

A chitosan stock solution of 7.5 mg/ml was prepared by dissolving chitosan in 10 mmol/l acetate solution. The Maillard reaction product (BSA–dextran conjugate) was freshly dissolved in water. The two solutions were mixed to reach a weight ratio of chitosan to BSA 0.1 and a desired final BSA concentration (0.5–5 mg/ml). After stirring for 2 h, the pH of the mixture was adjusted to 5.6. Then, the mixture solution was heated at 80 °C for 1 h. The resultant nanoparticle dispersion solution, nanoparticle solution in short, was kept at 4 °C before use. For the purpose of simplifying the description, in this paper, BSA concentrations in the conjugate and nanoparticle solutions were presented to denote the conjugate and nanoparticle concentrations, respectively.

2.4. Analysis of assembly efficiency of BSA–dextran–chitosan nanoparticles

After nanoparticle preparation, the free BSA and chitosan concentrations in the solution were analyzed. The nanoparticles were separated by ultracentrifugation of 154,000 × g at 4 °C for 90 min. The free BSA including free BSA–dextran conjugate concentration in the supernatant was analyzed by Coomassie brilliant blue assay (Sapan et al., 1999) and calibrated by BSA–dextran conjugate working curve. The free chitosan concentration in the supernatant was analyzed by alizarin red assay (Gao et al., 2003) and calibrated by chitosan working curve. Our control experiment confirmed that dextran in the solution does not influence chitosan analysis.

2.5. BSA–dextran–chitosan nanoparticle characterization

Dynamic laser scattering (DLS) measurements were carried out on a commercial laser light scattering instrument (Malvern Autosizer 4700, Malvern Instruments) at 25.0 °C and 90° scattering angle. The measured time correlation function was analyzed by the automatic program equipped with the correlator. The average hydrodynamic diameter (D_h) and polydispersity index (PDI, μ_2/Γ^2) were obtained by CONTIN mode analysis (Yuan et al., 2005; Zhang et al., 2005). The nanoparticle solutions were diluted to BSA concentration of 0.17 mg/ml for DLS measurements.

Atomic force microscopy (AFM) images were acquired in tapping mode on a Digital Instruments Nanoscope IV (Veeco Instruments) equipped with a silicon cantilever of 125 μm and an E-type vertical engage piezoelectric scanner. AFM sample was prepared by drying the nanoparticle solution on a freshly cleaved mica surface in a desiccator containing dried silica gel at room temperature for 2 days.

ζ-Potential measurements were performed on a ZetaSizer Nano ZS90 (Malvern Instruments). Electrophoresis mobility was measured and zeta potential ζ was calculated by the Dispersion Technology Software provided by Malvern according to Henry equation: $U_E = (2\varepsilon\zeta/3\eta)f(\text{ka})$, where ε, η, $f(\text{ka})$ are the dielectric permittivity of the solvent, viscosity of the solution, and Henry's function (Deshiikan and Papadopoulos, 1998). The nanoparticle sample for ζ-potential measurement was prepared by centrifugation then washing with water repeatedly to remove free chitosan, BSA and the conjugates in the solution.

2.6. Doxorubicin encapsulation

Doxorubicin hydrochloride solid powder or aqueous solution was added into the nanoparticle solution to reach a weigh ratio of doxorubicin to BSA 1:4, 1:2, or 1:1. The final BSA concentration was 4 mg/ml. After stirring in the dark for 12 h, the pH of the mixture was adjusted to 7.4–8.2. Then the mixture was stirred in the dark for another 24 h. The free doxorubicin in the solution was separated from the nanoparticles by a high-flow ultrafiltration membrane (cutoff M_w 30 kDa; MicroconYM-30, Millipore) and was collected in ultrafiltrate. The ultrafiltrate was mixed with PBS buffer (0.01 mol/l pH 7.4 phosphate buffer containing 0.15 mol/l NaCl) and then the absorbance at 480 nm was measured (Lambda 35, Perkin-Elmer) to analyze the free doxorubicin concentration. The adsorption of doxorubicin on the ultrafiltration membrane was calibrated by a standard free doxorubicin solution at the same condition.

2.7. Doxorubicin release in vitro

Doxorubicin loaded nanoparticle solution of 0.5 ml was dialyzed (cutoff M_w 14 kDa) against 24.5 ml release buffer at 37 °C. Periodically, a 3 ml of the release buffer was taken out and the same volume of fresh buffer was added. The absorbance at 480 nm was measured to analyze the doxorubicin concentration in the release buffer. The release experiments were repeated three times and average data were reported.

2.8. In vitro cytotoxicity

Cytotoxicity of BSA–dextran–chitosan nanoparticles and doxorubicin loaded nanoparticles against human non-small cell lung cancer A549 cell line was investigated by SRB (sulforhodamine B) assay (Houghton et al., 2007; Skehan et al., 1990). Briefly, the cells were seeded in 96-well plates with a density of 5×10^3 cells/well. The cells were grown in RPMI-1640 medium containing 10% calf serum, 250 mg/l gentamicin, and 25 mg/l amphotericin B. Cells were maintained at 37 °C in a humidified and 5% CO_2 incubator. After 24 h, cells were treated in triplicate with grade concentrations of the nanoparticle solution, doxorubicin loaded nanoparticle solution, and free doxorubicin solution for another 72 h. Then, the cells were fixed with 50 μl of 10% (w/v) ice-cold trichloroacetic acid for 1 h at 4 °C, washed with water for five times and air-dried. A 50 μl of 0.4% (w/v) SRB solution prepared with 1% (v/v) acetic acid was added to each well of the plates. After 30 min of staining at room temperature, the unbound SRB was removed by washing the plates with 1% (v/v) acetic acid for four times. Adding 150 μl of 10 mmol/l pH 10.5 Tris solution to each well solubilizes the bound SRB. The optical density (OD) of each well of the plates was read in a 96-well plate reader (DG3022) with the working wavelength of 520 nm. The three data of each sample at the same concentration were averaged. The cell growth inhibition rate (CIR) was calculated by the equation: CIR (%) = [(blank OD − sample OD)/blank OD] × 100.

2.9. In vivo antitumor efficacy

All the animal experiments of this report were performed at National Pharmaceutical Engineering Research Center in full compliance with the guidelines approved by Shanghai Administration of Experimental Animals [license no. SYXK (Shanghai) 2004–0015]. Kunming mice (18–22 g) from Shanghai Slac Laboratory Animal Co. Ltd. [license no. SCXK (Shanghai) 2003–0003] were subcutaneously injected in right axilla with 3×10^6 murine ascites hepatoma H22 cells. The mice were randomly assigned to various treatment groups with 5 male and 5 female in each group. The treatments were started after 3 days of the inoculation. Physiological saline, free doxorubicin and doxorubicin loaded nanoparticle solutions were intravenously injected via the tail veins, separately, with doxorubicin doses of 0–12 mg kg^{-1} d^{-1} for 5 days. After 10 days of the inoculation, all mice were sacrificed by cervical dislocation. The solid tumors were taken out and weighed. The tumor inhibition rate (TIR) was calculated by the equation: TIR (%) = (1 − WT/WC) × 100, where WT is the average tumor weight of doxorubicin treatment group, and WC is the average tumor weight of blank (physiological saline treatment) group.

For survivability study, Kunming mice were subcutaneously injected in abdomen with 2.4×10^6 murine ascites hepatoma H22 cells. The mice were randomly assigned to various treatment groups with 5 male and 5 female in each group. The treatments were started after 5 days of the inoculation. Physiological saline, free doxorubicin and doxorubicin loaded nanoparticle solutions were intravenously injected via the tail veins, separately, with doxorubicin doses of 0–12 mg kg^{-1} d^{-1} for 5 days. The survivable time of the mice were recorded. The survivability rate (SR) was calculated by the equation: SR (%) = $(T/C - 1) \times 100$, where T is the average survivable time of the doxorubicin treatment group and C is the average survivable time of blank group.

3. Results and discussion

3.1. BSA–dextran conjugate preparation

Maillard reaction is a natural and nontoxic process, which conjugates polysaccharide and protein by linking the reducing end carbonyl group in the former to the amino group in the latter (Dickinson and Semenova, 1992; Jimenez-Castano et al., 2007; Jung et al., 2006). BSA–dextran conjugates prepared through the Maillard reaction have been reported by several groups. The structure of BSA is not significantly disrupted after the reaction (Jung et al., 2006). BSA–dextran conjugates exhibit higher solubility and thermal stability than the native protein at the pH around BSA isoelectric point (Jimenez-Castano et al., 2007). In this study, BSA–dextran conjugates were prepared with the molar ratios of BSA to dextran (MR) 4:1, 2:1 and 1:1 under the condition reported previously by ourselves (Pan et al., 2006) and others (Jimenez-Castano et al., 2007; Jung et al., 2006). The conjugation degrees of the resultant conjugates were analyzed by sodium dodecyl sulfate-polyacrylamide gel electrophoresis and the standard gray scale method (Supplementary material). The analysis reveals that about 22.6%, 39.4% and 44.6% of the BSA was conjugated with dextran in the MR 4:1, 2:1 and 1:1 mixture, respectively.

3.2. BSA–dextran–chitosan nanoparticle preparation

3.2.1. Effect of the conjugates with different conjugation degrees

The pK_a of chitosan is 6.2–7.0 (Janes et al., 2001) and the isoelectric point of BSA is pH 4.8 (Lu et al., 2006). There is electrostatic attraction between chitosan and BSA in the pH range of 4.8–9 where they carry opposite charges that was verified by ζ-potential study below. Nanoparticles formed after heating chitosan and BSA mixture solution at pH around 5.6 by virtue of the electrostatic attraction and gelation of BSA, which is almost the same as our previous report of chitosan and ovalbumin mixture (Yu et al., 2006). However, the steric hindrance of the dextran in the conjugates can influence the electrostatic attraction between chitosan and BSA, and also influence the gelation ability of BSA. The effects of the conjugates with three different conjugation degrees on the nanoparticle formation were investigated. The weight ratio of chitosan to total BSA in the conjugates was fixed at 0.1 and total BSA concentration of the conjugates was 0.5 mg/ml. DLS result shows that the mixtures of chitosan and the conjugates having conjugation degrees of 22.6% and 39.4% can form nanoparticles after heat treatment at pH 5.6; the particle sizes are 164 and 131 nm, respectively. However, the particles prepared from the conjugates with 22.6% conjugation degree aggregate when adjusting the particle solution from acidic to neutral pH. This result suggests that the dextran on the particle surface is not enough to stabilize the particles in the pH range where chitosan is unprotonated. For the conjugates with the conjugation degree of 44.6%, almost no particles were detected after heating the mixture, indicating that too many dextran chains suppress the formation of the particles. In the following study, we used the conjugates with the conjugation degree of 39.4%, which contains 60.6% free BSA and 39.4% BSA–dextran conjugates, to prepare BSA–dextran–chitosan nanoparticles.

3.2.2. Effect of pH

The charges of chitosan and BSA carried are pH dependent, and therefore the electrostatic attraction between chitosan and the conjugates is also pH dependent. DLS result (Fig. 1) shows that the nanoparticles form after heating the mixture solutions in the pH

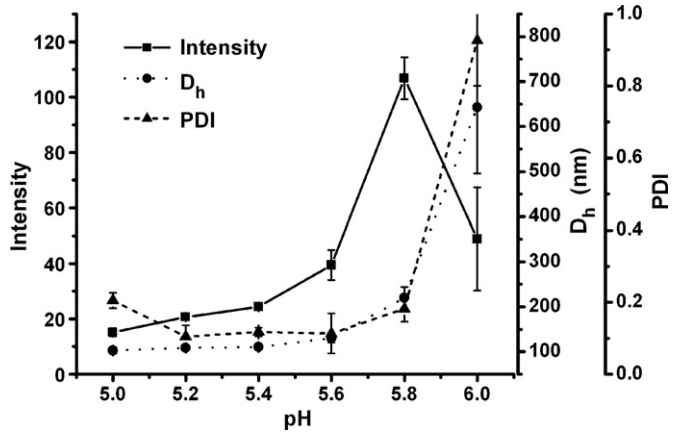

Fig. 1. DLS result of the nanoparticles produced by heating the mixture of chitosan and the conjugates at different pH values. The weight ratio of chitosan to total BSA in the conjugates was 0.1 and the BSA concentration was 0.5 mg/ml, $n = 3$.

range of 5–6. When the pH value changes from 5.0 to 5.6, the scattering light intensity increases, while the D_h value does not change significantly, indicating an increase of the particle number. Further increasing pH from 5.6 to 6.0, the D_h increases sharply and the intensity decreases after reaching its maximum at pH 5.8. Precipitates occurred when the pH of the mixture solution exceeded 6.0, which can be explained by the fact that some of the amino groups of chitosan are unprotonated and the solubility of chitosan decreases. On the other hand, both of chitosan and the conjugates carry positive charges when the pH of the solution is below 4.8. At the concentration of BSA 0.5 mg/ml, almost no particles formed after heating the mixture at pH 4.8. The data in Fig. 1 show that heating the mixture at pH 5.6, the D_h and PDI values of the resultant particles are relatively smaller. Therefore, we chose at pH 5.6 to heat the mixture of chitosan and the conjugates for particle preparation in the following study.

3.2.3. Effect of weight ratio of chitosan to the conjugates

Fig. 2 shows that the particle size distribution does not change significantly when the weight ratios of chitosan to the total BSA in the conjugates (WR) are in the range of 0.1–0.4 and the BSA concentration is 0.5 mg/ml. However, when increasing the chitosan ratio from 0.1 to 0.4, the free chitosan in the particle solution increases from 22% to 71% compared with the chitosan in feed, i.e., most of the increased chitosan does not assemble. Meanwhile, no free BSA was

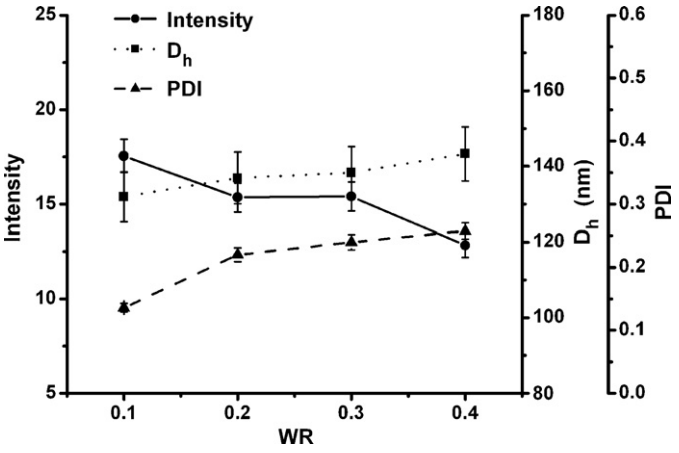

Fig. 2. DLS result of the nanoparticles produced with different weight ratios of chitosan to total BSA in the conjugates (WR). The BSA concentration was 0.5 mg/ml, $n = 3$.

Table 1
DLS result of BSA–dextran–chitosan nanoparticles prepared with different BSA concentrations, $n = 3$.

BSA concentration (mg/ml)	D_h (nm)	PDI
0.5	131 ± 11	0.12 ± 0.05
1	124 ± 4	0.15 ± 0.04
2.5	167 ± 14	0.25 ± 0.05
5	226 ± 12	0.24 ± 0.05

detected in the particle solutions in this WR range. In the following study, WR 0.1 was used to prepare the particles.

3.2.4. Effect of conjugate concentration

As indicated above, BSA concentrations were used to denote the conjugate and particle concentrations in this report. Table 1 shows that increasing the BSA concentration from 0.5 to 1 mg/ml does not cause significant change of the particle size distribution. Further increasing the BSA concentration to 2.5 and 5 mg/ml results in the increase of D_h to 167 and 226 nm, respectively; the PDI increases to about 0.25. In the following study, we used the nanoparticles with the BSA concentration of 5 mg/ml to load doxorubicin.

3.3. BSA–dextran–chitosan nanoparticle characterization

3.3.1. Stability of the nanoparticles in physiological condition

The nanoparticles prepared at the optimal condition, i.e., heating the mixture of chitosan and the conjugates at pH 5.6 with the weight ratio of chitosan to BSA 0.1, are very stable in PBS buffer. Two kinds of chitosan, M_w 50 kDa and deacetylation degree 95.5% as well as M_w 80–190 kDa and deacetylation degree 85%, were used to prepare the nanoparticles, while the dextran used has M_w 62 kDa. As shown in Table 2, the nanoparticle size distributions do not change significantly after changing the media to PBS buffer and then a month of storage.

3.3.2. Morphology of the nanoparticles

The morphology of the nanoparticles was observed by AFM. Fig. 3 exhibits that the nanoparticles are spherical with a smooth surface. The average diameter of the nanoparticles in Fig. 3 is 110 ± 39 nm and the average height is 23 ± 12 nm. The particle size obtained from AFM is much smaller than the size obtained from DLS, about 226 nm of the hydrodynamic diameter. As we know, DLS provides the data of the particles swollen in solution, while AFM shows the images of the particles spread and dried on a mica surface. The height is much smaller than the diameter, suggesting that the nanoparticles are soft and collapsed on the mica surface.

3.3.3. ζ-Potential

ζ-Potential is directly related to the net charges on the surface of the macromolecules and particles (Murray and Snowden, 1995). Fig. 4 displays that chitosan carries positive charges when the solution pH is lower than 9. BSA and the conjugates carry positive or negative charges when the pH of the solutions is lower or higher than 4.8; they show zero ζ-potential at pH 4.8, where is the isoelectric point of BSA. The absolute ζ-potential values of the conjugates are smaller than those of BSA. This phenomenon can be explained by the fact that the highly hydratable

Table 2
DLS result of BSA–dextran–chitosan nanoparticles in PBS buffer after storage. The nanoparticles were prepared at 0.5 mg/ml BSA concentration, $n = 3$.

Chitosan M_w (kDa)	Sample	D_h (nm)	PDI
50	Fresh prepared	131 ± 11	0.12 ± 0.05
	In PBS for a month	134 ± 13	0.27 ± 0.05
80–190	Fresh prepared	144 ± 12	0.25 ± 0.05
	In PBS for a month	129 ± 7	0.19 ± 0.09

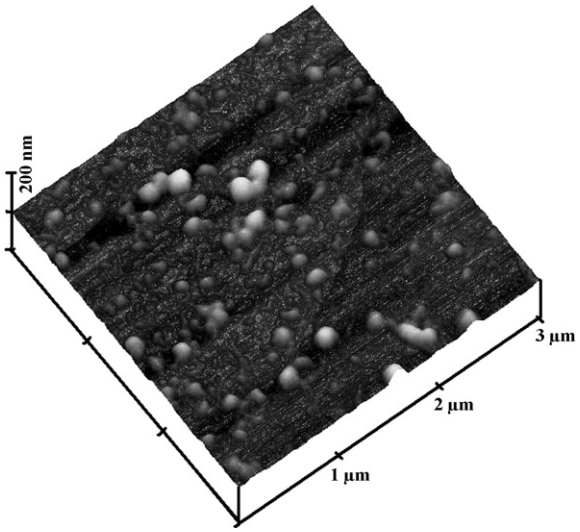

Fig. 3. AFM image of BSA–dextran–chitosan nanoparticles produced with 5 mg/ml BSA concentration.

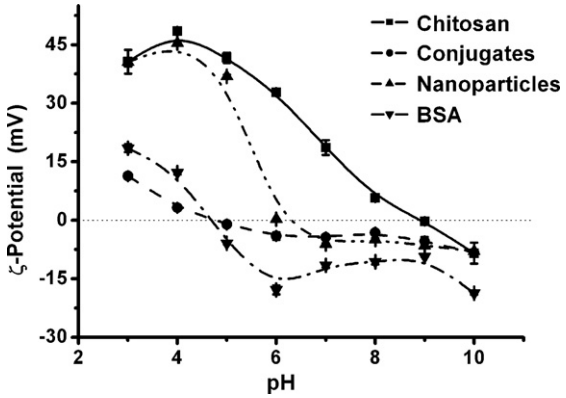

Fig. 4. pH dependence of the ζ-potentials of BSA, chitosan, BSA–dextran conjugates, and BSA–dextran–chitosan nanoparticles produced with 5 mg/ml BSA concentration.

dextran conjugated to BSA lowers the electrophoresis mobility of the conjugates. For the nanoparticle sample, the free chitosan and BSA and conjugates in the solution were separated before ζ-potential measurement. At pH around 4, the ζ-potential values of the nanoparticles are close to the values of chitosan, and they are much larger than the values of the conjugates. This result indicates that the protonated chitosan chains in acidic condition are extended in the shell of the particles. The particles carry about zero or negative charges when the pH of the solution is 6.0 or higher, respectively. The reason may be that the unprotonated chitosan shrinks and the charges of BSA on the core surface exert their effect.

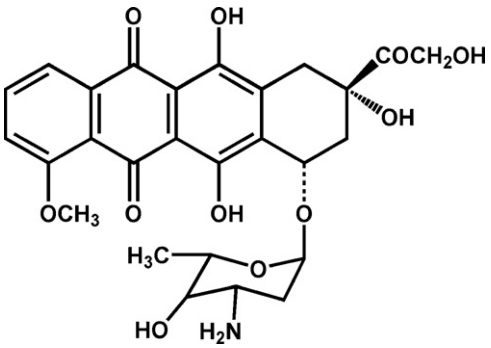

Scheme 2. Structure of doxorubicin.

3.4. BSA–dextran–chitosan nanoparticle formation mechanism

Our previous work verified that heating a mixture of chitosan and ovalbumin at pH 5.4 can produce nanoparticles with chitosan/ovalbumin core and chitosan shell that results in the aggregation of the nanoparticles at pH 7.4 (Yu et al., 2006). Therefore, the applications of chitosan–ovalbumin nanoparticles are limited. In this study, the assembly of chitosan with BSA–dextran conjugates produces long-term stable nanoparticles in PBS buffer, which demonstrates that the dextran chains conjugated to BSA are on the surface of the nanoparticles that increase the stability of the nanoparticles. As discussed above, about 60.6% of the BSA does not conjugate with dextran after the Maillard reaction. These individual BSA molecules can gelate after the heat treatment, forming the core of the nanoparticles. The BSA molecules conjugated with dextran locate on the surface of the nanoparticle core and the dextran chains extend in the shell of the nanoparticles, which is similar as the nanogels produced from lysozyme–dextran conjugates (Li et al., 2008). Chitosan chains are partly trapped in the nanoparticle core after heating because of the electrostatic attraction between chitosan and BSA that exists before and after the heat treatment. The rest of the chitosan chains extend in the shell of the nanoparticles, which is supported by the ζ-potential results of Fig. 4. The dextran and chitosan prevent BSA from macroscopically coagulating during the heat treatment at pH 5.6, and therefore chitosan and the conjugates assemble to the nanoparticles with chitosan/dextran shell and BSA/chitosan core. Scheme 1 illustrates the mechanism of the nanoparticle formation.

3.5. Doxorubicin loading into the nanoparticles

Scheme 2 shows the structure of doxorubicin. The pK_a of doxorubicin is 8.2 (Yang et al., 2000). The hydrophobicity/hydrophilicity and solubility of doxorubicin are pH dependent.

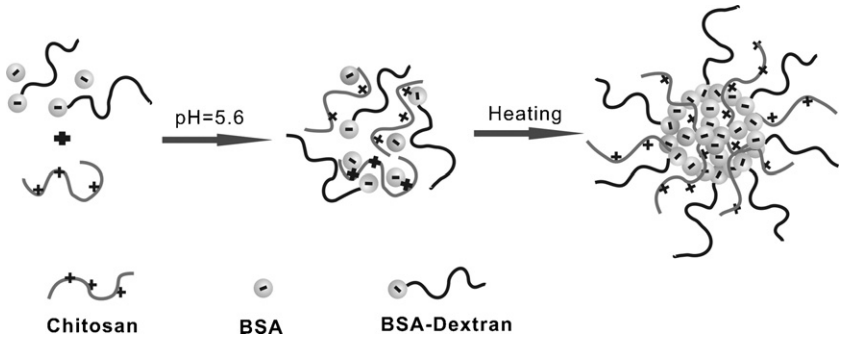

Scheme 1. Illustration of the formation of BSA–dextran–chitosan nanoparticles.

Table 3
Influences of the weight ratio of doxorubicin to BSA and the solution pH on the loading of doxorubicin into the nanoparticles.

Doxorubicin:BSA (w:w)	pH	Loading efficiency (%)	Loading amount (%)
1:4	7.4	71.8 ± 8.8[a]	12.1 ± 1.4[a]
1:2	7.4	57.9 ± 4.6	19.6 ± 1.5
1:1	7.4	61.7 ± 2.8[a]	41.7 ± 1.8[a]
1:1	7.9	70.0	47.3
1:1	8.2	82.6 ± 7.8[a]	55.8 ± 5.0[a]

[a] $n = 3$.

Protonated doxorubicin which carries a positive charge is soluble (10 mg/ml), whereas unprotonated one is insoluble in aqueous solution. The pyrene fluorescence demonstrates that the nanoparticles are relatively hydrophobic in the pH range of 2–10 (Supplementary material). It was reported that albumin is a natural carrier of hydrophobic molecules (Hawkins et al., 2008). So, doxorubicin can interact with the nanoparticles by hydrophobic interactions. Furthermore, the nanoparticles carry net negative charges when the solution pH is higher than 6.0 (Fig. 4). The electrostatic attraction between protonated doxorubicin and the nanoparticles happens when the solution pH changes from weak acidic to neutral or weak alkaline condition.

The loading of doxorubicin into the nanoparticles was performed by diffusion. The original pH of doxorubicin and the nanoparticle mixture was about 5. Then the pH of the mixture was changed to 7.4, 7.9 or 8.2, separately. The final BSA concentration was 4 mg/ml, i.e., the final nanoparticle concentration was 5.92 mg/ml (concentration sum of BSA, dextran and chitosan in the nanoparticles). The free doxorubicin in the nanoparticle solution after loading was separated by ultrafiltration and the doxorubicin concentration in the ultrafiltrate was analyzed. Doxorubicin loading efficiency and loading amount in the nanoparticles were calculated by the following equations:

$$\text{Loading efficiency (\%, w/w)} = \frac{\text{doxorubicin in feed} - \text{free doxorubicin}}{\text{doxorubicin in feed}} \times 100$$

$$\text{Loading amount (\%, w/w)} = \frac{\text{doxorubicin in feed} - \text{free doxorubicin}}{\text{nanoparticles in feed}} \times 100$$

Table 3 shows that increasing loading pH results in the increases of both loading efficiency and loading amount. This result is reasonable because increasing the solution pH from about 5 to 7.4 causes the increases of hydrophobic interactions and electrostatic attraction between doxorubicin and the nanoparticles as discussed above. Further increasing the solution pH to 8.2 can further increase the hydrophobic interactions. However, our HPLC analysis demonstrated that free doxorubicin decomposes in pH 8.2 solution, whereas it is stable in pH 7.4 solution (data not shown). Therefore, we chose at pH 7.4 to load doxorubicin into the nanoparticles. The data in Table 3 exhibit that increasing weight ratio of doxorubicin to BSA from 1:4 to 1:1 results in an increase of the loading amount but a decrease of the loading efficiency.

DLS measurement exhibits that the D_h of doxorubicin loaded nanoparticles (weight ratio of doxorubicin to BSA 1:1) is 328 nm with PDI 0.17, which is much larger than the 226 nm of the particles before loading (Table 1). After removing the unloaded doxorubicin by dialysis, the morphology of the loaded nanoparticles was observed by AFM. The image in Fig. 5 shows the loaded particles keep smooth surface and spherical shape. The loaded particles have average diameter of 120 ± 46 nm and average height of 23 ± 11 nm, which are very close to the particles before doxorubicin loading (Fig. 3). The loaded nanoparticles in Fig. 5 exhibit somewhat aggregation that may cause the increase of D_h in the solution. On the other hand, the loaded nanoparticles can pass through a membrane filter with 0.45 μm pore size and can be used as a sterile product.

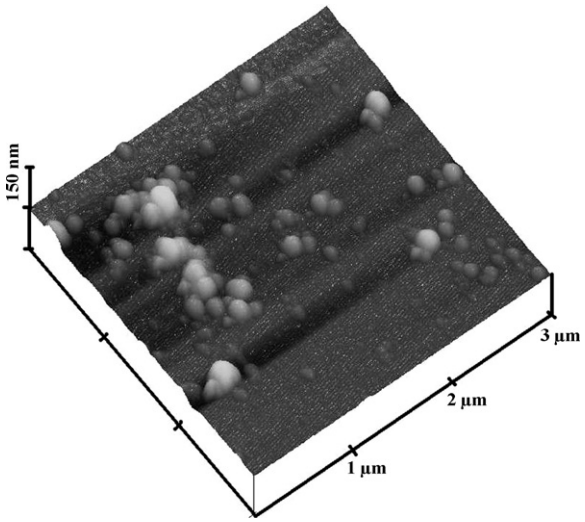

Fig. 5. AFM image of doxorubicin loaded nanoparticles. The loading was performed with doxorubicin and BSA concentrations of 1 and 4 mg/ml, respectively.

3.6. In vitro doxorubicin release from the nanoparticles

Fig. 6 shows the releases of doxorubicin from the nanoparticles in pH 7.4 PBS buffer and 0.1 mol/l pH 5.0 acetate buffer. Free doxorubicin solution was used as a control. The doxorubicin nanoparticles exhibit slower releases in both acetate and PBS buffers compared to the diffusions of free doxorubicin. Both of free doxorubicin and doxorubicin nanoparticles exhibit faster diffusion/release in pH 5.0 acetate buffer than their diffusion/release in pH 7.4 PBS buffer. This phenomenon can be explained by the fact that the protonated doxorubicin has a higher solubility. Besides, the hydrophobic interactions decrease as well as the electrostatic repulsion exists between the nanoparticles and doxorubicin at pH 5.0 as discussed above. The pH sensitive property of the nanoparticles may benefit the doxorubicin release in tumor cells whose pH is lower than the normal cells (Bae et al., 2003).

3.7. In vitro cytotoxicity of doxorubicin nanoparticles

The cytotoxicities of the unloaded nanoparticles, doxorubicin loaded nanoparticles, and free doxorubicin against human non-small cell lung cancer A549 cell line were investigated. The free

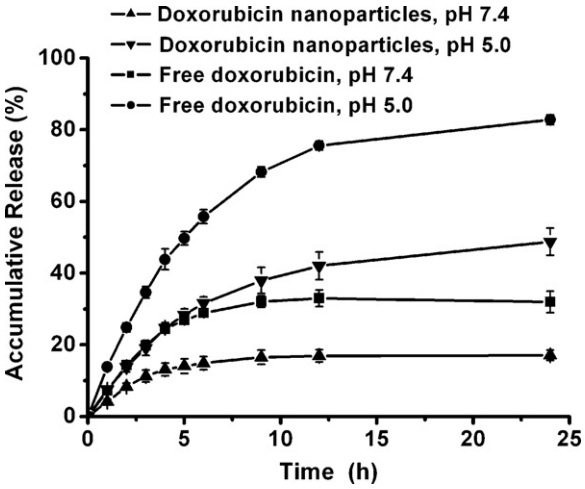

Fig. 6. Accumulative release of doxorubicin from doxorubicin loaded nanoparticles in 0.1 mol/l pH 5.0 acetate buffer and pH 7.4 PBS buffer. The free doxorubicin was used as a control.

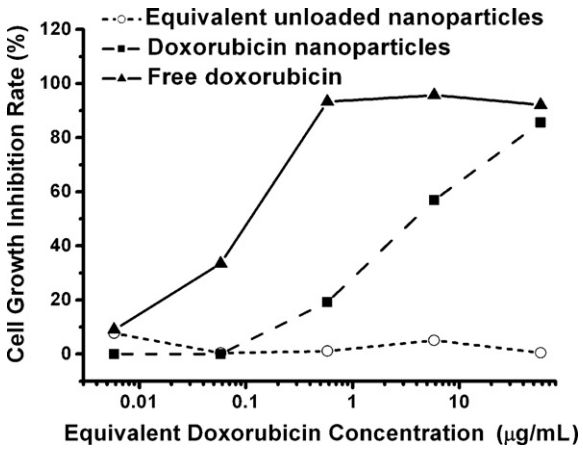

Fig. 7. Cell inhibition effects of free doxorubicin, doxorubicin loaded nanoparticles and equivalent unloaded nanoparticles, i.e., the unloaded nanoparticles containing the same BSA, dextran and chitosan concentrations as the doxorubicin nanoparticles.

doxorubicin in the nanoparticle solution was removed by dialysis. Fig. 7 displays that free doxorubicin inhibits the cell growth more than 90% when its concentration is 0.58 μg/ml, which is 2 orders of magnitude smaller than equivalent 58 μg/ml doxorubicin of the loaded nanoparticles which exhibit the same effect. It is possible that the slower release of the loaded doxorubicin reduces the cytotoxicity of doxorubicin nanoparticles. The unloaded nanoparticles with the same equivalent concentration, i.e., containing the same BSA, dextran and chitosan concentrations as the doxorubicin nanoparticles, have no cytotoxicity. This result confirms that BSA–dextran–chitosan nanoparticles are completely biocompatible.

3.8. In vivo antitumor effect of doxorubicin nanoparticles

The effects of doxorubicin nanoparticles on the treatment of murine ascites hepatoma H22 tumor-bearing mice were investigated. The data in Table 4 exhibit that the tumor inhibition rates of the doxorubicin nanoparticle are lower than the free doxorubicin at the same dose. On the other hand, the nanoparticle treatment groups with 3, 5, and 8 mg/kg doses of doxorubicin do not decrease the body weights, whereas the 5 mg/kg dose of free doxorubicin group decreases the body weight badly. These results mean that the activity and toxicity of the doxorubicin nanoparticles are smaller than free doxorubicin. It is possible that the delayed release of the doxorubicin from the nanoparticles results in the decreases of the activity and toxicity. Further increasing the nanoparticle dose to equivalent 12 mg/kg doxorubicin causes the toxicity increases, but the tumor inhibition rate does not improve.

Table 5
Survivability of hepatoma H22 tumor-bearing mice after the treatments with free doxorubicin and doxorubicin nanoparticles.

Group	Average life time	Survivability rate (%)
Blank 1	10.4 ± 2.2	
Blank 2	10.3 ± 1.8	
Free doxorubicin (5 mg/kg)	11.2 ± 1.7[a]	8.21
Doxorubicin nanoparticles (doxorubicin 12 mg/kg)	14.8 ± 4.0[b]	43.0

[a] $P > 0.05$ compared with blank group 2.
[b] $P < 0.01$ compared with blank group 2.

Table 6
Survivability of hepatoma H22 tumor-bearing mice after the treatments with free doxorubicin and doxorubicin nanoparticles containing 25% unloaded doxorubicin.

Batch	Group	Average life time	Survivability rate (%)
I	Blank 1	16.1 ± 1.5	
	Free doxorubicin (5 mg/kg)	16.3 ± 2.7[a]	1.24
	Doxorubicin nanoparticles (doxorubicin 5 mg/kg)	25.2 ± 6.4[b]	56.5
II	Blank 2	14.7 ± 1.6	
	Blank 3	14.3 ± 0.8	
	Free doxorubicin (5 mg/kg)	13.7 ± 1.4[c]	–
	Doxorubicin nanoparticles (doxorubicin 8 mg/kg)	21.3 ± 1.6[d]	46.9

[a] $P > 0.05$ compared with blank group 1.
[b] $P < 0.01$ compared with blank group 1.
[c] $P > 0.05$ compared with blank group 3.
[d] $P < 0.01$ compared with blank group 3.

In order to further investigate the antitumor effects of the nanoparticles, the survival studies of murine ascites hepatoma H22 tumor-bearing mice were performed. The treatment of the nanoparticles with doxorubicin dose of 12 mg/kg prolonged the life of the tumor-bearing mice from 10.3 to 14.8 days; the survivability rate is 43.0%, which is significantly higher than the treatment of 5 mg/kg dose of free doxorubicin (Table 5). This result proves that the nanoparticles are more effective than free doxorubicin to prolong the life of the tumor-bearing mice.

Kratz pointed that only the free drug could exert its pharmacological effect (Kratz, 2008). Therefore, we speculated that the mixture of loaded and unloaded doxorubicin may increase the antitumor effects, i.e., the unloaded doxorubicin can increase the tumor inhibition rate, while the extended doxorubicin release and the passive tumor target of the nanoparticles can reduce the toxicity and increase the doxorubicin concentration in tumor tissue. We used the doxorubicin nanoparticle solution containing 25% unloaded doxorubicin to investigate the antitumor effects. The result in Table 6 shows the survivability rates of the tumor-bearing mice are 56.5% and 46.9% after the treatments with the nanoparticles of 5 and 8 mg/kg doses of doxorubicin, respectively, while the

Table 4
Tumor inhibition effects of free doxorubicin and doxorubicin nanoparticles on hepatoma H22 tumor-bearing mice.

Batch	Group	Mice number (beginning/end)	Average body weight (g, beginning/end)	Average tumor weight (g)	Tumor inhibition rate (%)
I	Blank 1	10/10	19.9/25.2	3.17 ± 0.58	
	Free doxorubicin (3 mg/kg)	10/10	20.1/20.9	1.78 ± 0.43[a]	43.9
	Free doxorubicin (5 mg/kg)	10/10	19.7/15.9	0.86 ± 0.22[a]	72.9
	Doxorubicin nanoparticles (doxorubicin 3 mg/kg)	10/10	20.0/23.9	2.28 ± 0.25[a]	28.1
	Doxorubicin nanoparticles (doxorubicin 5 mg/kg)	10/10	20.1/23.1	2.11 ± 0.50[a]	33.4
	Doxorubicin nanoparticles (doxorubicin 8 mg/kg)	10/10	19.9/21.9	1.69 ± 0.29[a]	46.7
II	Blank 2	10/10	21.2/23.0	2.77 ± 0.61	
	Free doxorubicin (5 mg/kg)	10/10	21.7/16.2	1.01 ± 0.34[b]	63.5
	Doxorubicin nanoparticles (doxorubicin 12 mg/kg)	10/9	21.3/20.4	1.84 ± 0.52[b]	33.6

[a] $P < 0.01$ compared with the blank group 1.
[b] $P < 0.01$ compared with the blank group 2.

group treated with 5 mg/kg free doxorubicin does not have positive survivability effect this time. Our antitumor studies verify that free doxorubicin is more effective to inhibit tumor growth, but is less effective to prolong the life of the tumor-bearing mice compared with the doxorubicin loaded nanoparticles.

4. Conclusions

BSA–dextran–chitosan nanoparticles were fabricated by heating the mixture of chitosan and BSA–dextran conjugates at pH 5.6 with a weight ratio of chitosan to total BSA in the conjugates 0.1. The conjugates having the conjugation degree of 39.4% were prepared by the Maillard reaction with a molar ratio of BSA to dextran 2:1. BSA molecules gelate forming the core of the nanoparticles after a heat treatment at pH 5.6. Chitosan chains are partly trapped in the nanoparticle core after heating because of the electrostatic attraction between chitosan and BSA. The rest of the chitosan and the dextran conjugated to BSA extend in the shell of the nanoparticles. The fabrication process of the nanoparticles is simple, green and low-cost. The resultant nanoparticles are stable in physiological condition and completely biocompatible.

Doxorubicin was effectively loaded into BSA–dextran–chitosan nanoparticles by diffusion when the pH of doxorubicin and the nanoparticle mixture was changed from 5 to 7.4. The loaded nanoparticles can largely decrease the toxicity of doxorubicin and significantly increase the survivability of hepatoma H22 tumor-bearing mice.

Acknowledgements

The financial supports of National Natural Science Foundation of China (NSFC Project 50673020), Science and Technology Committee of Shanghai Municipality (07DJ14004), and National Basic Research Program of China (973 Program 2009CB930400) are acknowledged.

Appendix A. Supplementary data

Supplementary data associated with this article can be found, in the online version, at doi:10.1016/j.ijpharm.2010.03.063.

References

Bae, Y., Fukushima, S., Harada, A., Kataoka, K., 2003. Design of environment-sensitive supramolecular assemblies for intracellular drug delivery: polymeric micelles that are responsive to intracellular pH change. Angew. Chem. Int. Ed. 42, 4640–4643.

Boye, J.I., Alli, I., Ismail, A.A., 1996. Interactions involved in the gelation of bovine serum albumin. J. Agric. Food Chem. 44, 996–1004.

Carvalho, C., Santos, R.X., Cardoso, S., Correia, S., Oliveira, P.J., Santos, M.S., Moreira, P.I., 2009. Doxorubicin: the good, the bad and the ugly effect. Curr. Med. Chem. 16, 3267–3285.

Choi, K.C., Bang, J.Y., Kim, C., Kim, P.I., Lee, S.R., Chung, W.T., Park, W.D., Park, J.S., Lee, Y.S., Song, C.E., Lee, H.Y., 2009. Antitumor effect of adriamycin-encapsulated nanoparticles of poly(DL-lactide-co-glycolide)-grafted dextran. J. Pharmacol. Sci. 98, 2104–2112.

Desai, N., Trieu, V., Yao, Z.W., Louie, L., Ci, S., Yang, A., Tao, C.L., De, T., Beals, B., Dykes, D., Noker, P., Yao, R., Labao, E., Hawkins, M., Soon-Shiong, P., 2006. Increased antitumor activity, intratumor paclitaxel concentrations, and endothelial cell transport of Cremophor-free, albumin-bound paclitaxel, ABI-007, compared with Cremophor-based paclitaxel. Clin. Cancer Res. 12, 1317–1324.

Deshiikan, S.R., Papadopoulos, K.D., 1998. Modified Booth equation for the calculation of zeta potential. Colloid Polym. Sci. 276, 117–124.

Dickinson, E., Semenova, M.G., 1992. Emulsifying properties of covalent protein dextran hybrids. Colloids Surf. 64, 299–310.

Dreis, S., Rothweller, F., Michaelis, A., Cinatl, J., Kreuter, J., Langer, K., 2007. Preparation, characterisation and maintenance of drug efficacy of doxorubicin-loaded human serum albumin (HSA) nanoparticles. Int. J. Pharm. 341, 207–214.

Ferry, J.D., 1948. Protein gels. Adv. Protein Chem. 4, 1–78.

Gabizon, A., Shmeeda, H., Barenholz, Y., 2003. Pharmacokinetics of pegylated liposomal doxorubicin—review of animal and human studies. Clin. Pharmacokinet. 42, 419–436.

Gao, G.Z., Jiao, Q.C., Liu, Q., Ding, Y.L., Chen, L., 2003. Study on the mechanism of the interaction between chitosan and alizarin red. Acta Chim. Sin. 61, 1294–1298.

Gref, R., Minamitake, Y., Peracchia, M.T., Trubetskoy, V., Torchilin, V., Langer, R., 1994. Biodegradable long-circulating polymeric nanospheres. Science 263, 1600–1603.

Hasegawa, M., Yagi, K., Iwakawa, S., Hirai, M., 2001. Chitosan induces apoptosis via caspase-3 activation in bladder tumor cells. Jpn. J. Cancer Res. 92, 459–466.

Hawkins, M.J., Soon-Shiong, P., Desai, N., 2008. Protein nanoparticles as drug carriers in clinical medicine. Adv. Drug Deliv. Rev. 60, 876–885.

Houghton, P., Fang, R., Techatanawat, I., Steventon, G., Hylands, P.J., Lee, C.C., 2007. The sulphorhodamine (SRB) assay and other approaches to testing plant extracts and derived compounds for activities related to reputed anticancer activity. Methods 42, 377–387.

Hu, Y., Ding, Y., Ding, D., Sun, M.J., Zhang, L.Y., Jiang, X.Q., Yang, C.Z., 2007. Hollow chitosan/poly(acrylic acid) nanospheres as drug carriers. Biomacromolecules 8, 1069–1076.

Janes, K.A., Fresneau, M.P., Marazuela, A., Fabra, A., Alonso, M.J., 2001. Chitosan nanoparticles as delivery systems for doxorubicin. J. Control. Release 73, 255–267.

Jimenez-Castano, L., Villamiel, M., Lopez-Fandino, R., 2007. Glycosylation of individual whey proteins by Maillard reaction using dextran of different molecular mass. Food Hydrocolloids 21, 433–443.

Jung, S.H., Choi, S.J., Kim, H.J., Moon, T.W., 2006. Molecular characteristics of bovine serum albumin–dextran conjugates. Biosci. Biotechnol. Biochem. 70, 2064–2070.

Kratz, F., 2007. DOXO-EMCH (INNO-206): the first albumin-binding prodrug of doxorubicin to enter clinical trials. Expert Opin. Invest. Drugs 16, 855–866.

Kratz, F., 2008. Albumin as a drug carrier: design of prodrugs, drug conjugates and nanoparticles. J. Control. Release 132, 171–183.

Lemarchand, C., Gref, R., Couvreur, P., 2004. Polysaccharide-decorated nanoparticles. Eur. J. Pharm. Biopharm. 58, 327–341.

Li, C., Wallace, S., 2008. Polymer–drug conjugates: recent development in clinical oncology. Adv. Drug Deliv. Rev. 60, 886–898.

Li, J., Yu, S.Y., Yao, P., Jiang, M., 2008. Lysozyme–dextran core–shell nanogels prepared via a green process. Langmuir 24, 3486–3492.

Lu, B., Xiong, S.B., Yang, H., Yin, X.D., Zhao, R.B., 2006. Mitoxantrone-loaded BSA nanospheres and chitosan nanospheres for local injection against breast cancer and its lymph node metastases. I. Formulation and in vitro characterization. Int. J. Pharm. 307, 168–174.

Minotti, G., Menna, P., Salvatorelli, E., Cairo, G., Gianni, L., 2004. Anthracyclines: molecular advances and pharmacologic developments in antitumor activity and cardiotoxicity. Pharmacol. Rev. 56, 185–229.

Mitra, S., Gaur, U., Ghosh, P.C., Maitra, A.N., 2001. Tumour targeted delivery of encapsulated dextran–doxorubicin conjugate using chitosan nanoparticles as carrier. J. Control. Release 74, 317–323.

Murray, M.J., Snowden, M.J., 1995. The preparation, characterization and applications of colloidal microgels. Adv. Colloid Interface Sci. 54, 73–91.

Otsuka, H., Nagasaki, Y., Kataoka, K., 2003. PEGylated nanoparticles for biological and pharmaceutical applications. Adv. Drug Deliv. Rev. 55, 403–419.

Pan, X.Y., Mu, M.F., Hu, B., Yao, P., Jiang, M., 2006. Micellization of casein–graft–dextran copolymer prepared through Maillard reaction. Biopolymers 81, 29–38.

Park, J.H., Gu, L., von Maltzahn, G., Ruoslahti, E., Bhatia, S.N., Sailor, M.J., 2009. Biodegradable luminescent porous silicon nanoparticles for in vivo applications. Nat. Mater. 8, 331–336.

Passirani, C., Barratt, G., Devissaguet, J.P., Labarre, D., 1998. Long-circulating nanoparticles bearing heparin or dextran covalently bound to poly(methyl methacrylate). Pharm. Res. 15, 1046–1050.

Patil, R.R., Guhagarkar, S.A., Devarajan, P.V., 2008. Engineered nanocarriers of doxorubicin: a current update. Crit. Rev. Ther. Drug Carrier Syst. 25, 1–61.

Pereverzeva, E., Treschalin, I., Bodyagin, D., Maksimenko, O., Langer, K., Dreis, S., Asmussen, B., Kreuter, J., Gelperina, S., 2007. Influence of the formulation on the tolerance profile of nanoparticle-bound doxorubicin in healthy rats: focus on cardio- and testicular toxicity. Int. J. Pharm. 337, 346–356.

Purcell, M., Neault, J.F., Tajmir-Riahi, H.A., 2000. Interaction of taxol with human serum albumin. BBA-Protein Struct. Mol. Enzymol. 1478, 61–68.

Qi, L.F., Xu, Z.R., Chen, M.L., 2007. In vitro and in vivo suppression of hepatocellular carcinoma growth by chitosan nanoparticles. Eur. J. Cancer 43, 184–193.

Sapan, C.V., Lundblad, R.L., Price, N.C., 1999. Colorimetric protein assay techniques. Biotechnol. Appl. Biochem. 29, 99–108.

Skehan, P., Storeng, R., Scudiero, D., Monks, A., McMahon, J., Vistica, D., Warren, J.T., Bokesch, H., Kenney, S., Boyd, M.R., 1990. New colorimetric cytotoxicity assay for anticancer-drug screening. J. Natl. Cancer Inst. 82, 1107–1112.

Son, Y.J., Jang, J.S., Cho, Y.W., Chung, H., Park, R.W., Kwon, I.C., Kim, I.S., Park, J.Y., Seo, S.B., Park, C.R., Jeong, S.Y., 2003. Biodistribution and anti-tumor efficacy of doxorubicin loaded glycol–chitosan nanoaggregates by EPR effect. J. Control. Release 91, 135–145.

Tan, M.L., Choong, P.F.M., Dass, C.R., 2009. Review: doxorubicin delivery systems based on chitosan for cancer therapy. J. Pharm. Pharmacol. 61, 131–142.

Wattendorf, U., Merkle, H.P., 2008. PEGylation as a tool for the biomedical engineering of surface modified microparticles. J. Pharmacol. Sci. 97, 4655–4669.

Yang, S.C., Ge, H.X., Hu, Y., Jiang, X.Q., Yang, C.Z., 2000. Doxorubicin-loaded poly(butylcyanoacrylate) nanoparticles produced by emulsifier-free emulsion polymerization. J. Appl. Polym. Sci. 78, 517–526.

Yokoe, J.I., Sakuragi, S., Yamamoto, K., Teragaki, T., Ogawara, K.I., Higaki, K., Katayama, N., Kai, T., Sato, M., Kimura, T., 2008. Albumin-conjugated PEG liposome enhances tumor distribution of liposomal doxorubicin in rats. Int. J. Pharm. 353, 28–34.
Yu, S.Y., Hu, J.H., Pan, X.Y., Yao, P., Jiang, M., 2006. Stable and pH-sensitive nanogels prepared by self-assembly of chitosan and ovalbumin. Langmuir 22, 2754–2759.
Yuan, X.F., Harada, A., Yamasaki, Y., Kataoka, K., 2005. Stabilization of lysozyme-incorporated polyion complex micelles by the omega-end derivatization of poly(ethylene glycol)-poly(alpha,beta-aspartic acid) block copolymers with hydrophobic groups. Langmuir 21, 2668–2674.
Zhang, J., Chen, X.G., Li, Y.Y., Liu, C.S., 2007. Self-assembled nanoparticles based on hydrophobically modified chitosan as carriers for doxorubicin. Nanomedicine: Nanotechnol. Biol. Med. 3, 258–265.
Zhang, W.A., Zhou, X.C., Li, H., Fang, Y., Zhang, G.Z., 2005. Conformational transition of tethered poly(N-isopropylacrylamide) chains in coronas of micelles and vesicles. Macromolecules 38, 909–914.